JGR Biogeosciences

RESEARCH ARTICLE
10.1029/2020JG006008

Special Section:
The Arctic: An AGU Joint Special Collection

Permafrost Organic Carbon Turnover and Export Into a High-Arctic Fjord: A Case Study From Svalbard Using Compound-specific ^{14}C Analysis

Stephanie Kusch[1,2,5], Janet Rethemeyer[3], Daniela Ransby[1,4], and Gesine Mollenhauer[1,2]

[1]Alfred Wegener Institute for Polar and Marine Research, Bremerhaven, Germany, [2]Faculty of Geosciences, University of Bremen, Bremen, Germany, [3]University of Cologne, Institute of Geology and Mineralogy, Cologne, Germany, [4]MARUM – Center for Marine Environmental Sciences, University of Bremen, Bremen, Germany, [5]University of Cologne, CologneAMS, Cologne, Germany

Abstract In a warming climate, thawing permafrost soils in the circumpolar Arctic region are subject to enhanced microbial turnover as well as mass mobilization and other erosion processes. High-Arctic settings such as Svalbard are exceptionally vulnerable to these effects, but the presence of coal deposits obscures the organic carbon (OC) signature of permafrost OC, particularly its carbon isotope composition, when studying OC turnover and export. Here, we analyze the compound-specific $\delta^{13}C$ and $\Delta^{14}C$ isotopic composition of alkanoic acids from permafrost soils and river and fjord sediments to assess soil turnover in the catchment of the Bayelva River near Ny-Ålesund and trace transport and re-burial of permafrost OC into the adjacent Kongsfjord. Our data confirm the influence of coal-derived OC on $\delta^{13}C$ and $\Delta^{14}C$ values of bulk soil and sedimentary OC, while alkanoic acid $\delta^{13}C$ and $\Delta^{14}C$ values are less affected by coal contributions. Alkanoic acid $\Delta^{14}C$ values in the soil profile imply long–term residence in soils prior to deposition in river and fjord sediments, that is, multi-millennial turnover that is significantly slower than reported from other environments. Strongly ^{14}C-depleted vascular plant-derived long-chain alkanoic acids can be found in Bayelva River and Kongsfjord sediments revealing substantial input of deep active layer/permafrost OC, particularly in the Bayelva River and off its river mouth. In the central Kongsfjord, long-chain alkanoic acid $\Delta^{14}C$ values are higher either reflecting input from other permafrost areas or physical effects resulting, for example, from deposition in settings with different accumulation rates or from sediment sorting.

Plain Language Summary Rising atmospheric temperatures have a particularly strong effect on carbon cycling in high latitude ecosystems such as Svalbard. Thawing of permanently frozen ground (permafrost) results in stronger microbial activity as well as erosion and reburial of previously frozen old carbon-rich material in aquatic systems. Such processes are poorly constrained in Svalbard and can be studied using carbon isotope analyses and ^{14}C dating. However, permafrost carbon is difficult to identify in sediments due to the contribution of fossil carbon from coal. Therefore, molecular-level techniques are required.

Here, we use molecular-level carbon isotope analysis of lipids to study permafrost turnover and export in a river catchment and fjord system on Svalbard. Our results show that lipid turnover in permafrost soils is significantly slower than in other environments, likely as a result of the low mean annual temperature and precipitation. Moreover, our results imply erosion and reburial of substantial amounts of deep permafrost soil in river and fjord sediments although the sedimentary permafrost signal is spatially heterogenous. This spatial variability may be caused by recent soil temperature change or result from sedimentological processes.

Key Points:

- Permafrost turnover and export can be traced using alkanoic acid $\delta^{13}C$ and $\Delta^{14}C$ whereas bulk organic carbon (OC) isotope values are biased by coal-derived OC
- Alkanoic acid turnover in permafrost is multi-millennial likely controlled by low mean annual air temperature and precipitation
- Long-chain alkanoic acid $\Delta^{14}C$ values in river and fjord sediments imply reburial of deep active layer and permafrost OC

Supporting Information:

- Supporting Information S1
- Table S1
- Table S2

Correspondence to:
S. Kusch,
stephanie.kusch@uni-koeln.de

Citation:
Kusch, S., Rethemeyer, J., Ransby, D., & Mollenhauer, G. (2021). Permafrost organic carbon turnover and export into a high-Arctic fjord: A case study from Svalbard using compound-specific ^{14}C analysis. *Journal of Geophysical Research: Biogeosciences*, *126*, e2020JG006008. https://doi.org/10.1029/2020JG006008

Received 7 AUG 2020
Accepted 8 JAN 2021

Author Contributions:
Data curation: Daniela Ransby
Formal analysis: Stephanie Kusch, Janet Rethemeyer, Daniela Ransby

1. Introduction

Permafrost soils (perennially frozen ground) represent a huge reservoir of organic carbon (OC) storing approximately twice the amount of C found in the present-day atmosphere and accounting for roughly 50% of the global belowground OC reservoir (Hugelius et al., 2014; Tarnocai et al., 2009). In the deeper and permanently frozen permafrost layers (below the active layer thawing during summer

Funding acquisition: Gesine Mollenhauer
Methodology: Stephanie Kusch, Janet Rethemeyer
Resources: Gesine Mollenhauer
Supervision: Gesine Mollenhauer
Writing – original draft: Stephanie Kusch
Writing – review & editing: Stephanie Kusch, Janet Rethemeyer, Daniela Ransby, Gesine Mollenhauer

time), this OC is nearly inaccessible to microbial decomposition (Waldrop et al., 2010). However, circum-Arctic permafrost areas have experienced substantial warming during the last decades (Biskaborn et al., 2019; Christiansen et al., 2010; Romanovsky et al., 2010; S. L. Smith et al., 2010) causing permafrost thaw. Upon thaw, the OM stored in permafrost is susceptible to *in situ* microbial decomposition and enhanced mass erosion into aquatic systems including high-Arctic rivers and the Arctic Ocean (IPCC, 2013). While these aquatic systems may be characterized by even stronger microbial and photo-oxidative mineralization (Cory et al., 2013; Vonk et al., 2013), quick export of permafrost OM into marine sediments might act as efficient long-term CO_2 sink (Hilton et al., 2015). In particular, fjords in high latitudes have recently been shown to be globally important OC sinks, which may act as significant sequestration and reburial environments of mobilized permafrost OM (Cui et al., 2016; R. W. Smith et al., 2015).

Due to its particular vulnerability to warming, the high-Arctic area is of prime interest to study the quality of permafrost OC and to trace its export into fjords. Yet, substantial data gaps persist in permafrost distribution and carbon stocks for the high-Arctic region (Hugelius et al., 2014) including the Svalbard archipelago in the high European Arctic. Svalbard has experienced an unprecedented increase (ca. 2°C–3°C) of overall mean annual air temperatures during the 20th century (D'Andrea et al., 2012; Førland et al., 2011; Humlum et al., 2003; Maturilli & Kayser, 2016) and rising permafrost ground temperatures with deepening of the active layer since the 1990s (Boike et al., 2018; Christiansen et al., 2010; Isaksen et al., 2007). Accordingly, assessing OC turnover in Svalbard permafrost and characterizing and quantifying permafrost OC export into Svalbard fjords is a crucial baseline parameter to determine a potential acceleration of permafrost OC degradation/turnover and export in response to changing temperatures under Arctic amplification (Koven et al., 2015; Schädel et al., 2013, 2016; Schuur et al., 2009).

Dual carbon isotope (^{13}C and ^{14}C) analysis has been proven a powerful tool to study the quality and accessibility of permafrost OC (Dutta et al., 2006; Zimov et al., 2006) as well as the deposition of permafrost-derived OC in aquatic systems such as marine sediments (Winterfeld et al., 2015). The advantage of using a dual isotope approach lies in its ability to differentiate permafrost OC from other sources of OC such as marine production and/or to differentiate different permafrost deposit types (Dutta et al., 2006; Vonk et al., 2012; Winterfeld et al., 2015). However, the application of bulk ^{14}C is severely limited in environments influenced by contributions from fossil (^{14}C-free) OC sources such as kerogen or coal (Drenzek et al., 2007). On Svalbard, several coal-bearing strata primarily from the Carboniferous and Tertiary are exposed across the Spitsbergen island (Harland et al., 1976; Orvin, 1934). Accordingly, bulk $\Delta^{14}C$ values do not allow assessing OC turnover in permafrost soils and the multitude of endmembers contributing to bulk $\Delta^{14}C$ values in fjord sediments severely limits the characterization and quantification of reburied permafrost OC as it requires additional constraints to resolve mass balance calculations (e.g., Kim et al., 2011). To overcome these challenges, compound-specific radiocarbon analysis (CSRA) of vascular plant biomarkers such as alkanoic acids can be used. Long-chain alkanoic acids derive from the protective epicuticular wax cover of leaves (Eglinton & Hamilton, 1967) and they are commonly used as molecular evidence/proxies for terrestrial plants (for an overview see Diefendorf & Freimuth, 2017). CSRA of alkanoic acids has aided in understanding soil OC turnover (van der Voort et al., 2017) and has been successfully used to estimate mean residence times on the continent prior to delivery into aquatic settings (Drenzek et al., 2007; Kusch et al., 2010). In the Arctic, CSRA also has revealed the increased release and mobilization of permafrost OC in response to recent and deglacial warming (Feng et al., 2013; Meyer et al., 2019; Winterfeld et al., 2018). Yet, this tool has thus far not been used to study permafrost turnover (determined by the balance of preservation vs. degradation), in fact, only few studies to date report compound-specific alkanoic acid ^{14}C data from soils (Matsumoto et al., 2007; van der Voort et al., 2017). Moreover, compound-specific ^{14}C data along the land-to-ocean export continuum are as of yet missing from the high-Arctic (>70°N).

To study the quality and export of permafrost OC into a Svalbard fjord, we obtained compound-specific $\delta^{13}C$ and $\Delta^{14}C$ data from permafrost soils in the Bayelva River catchment as well as sediments from the Bayelva River and Kongsfjord, a well-studied natural laboratory. We use our compound-specific alkanoic acid isotope data to determine permafrost OC turnover in the Bayelva catchment, assess export mechanisms along the flow path, and characterize the spatial dispersal and reburial of permafrost OC in Kongsfjord sediments.

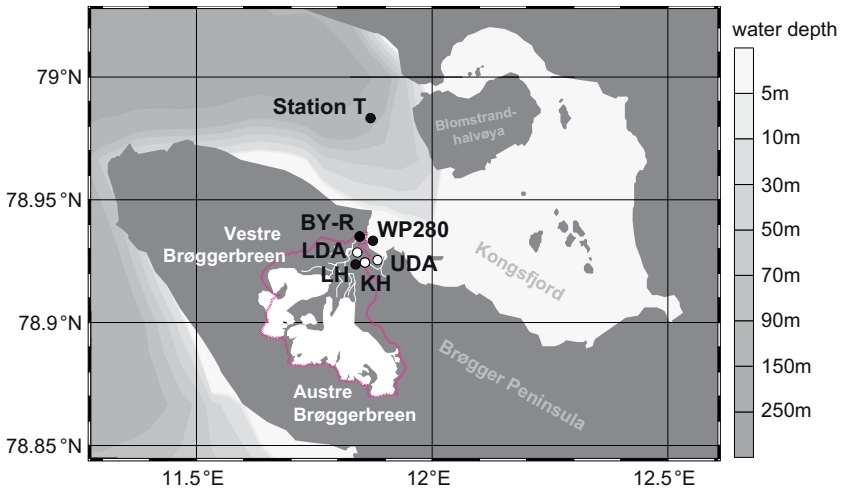

Figure 1. Study area with sampling locations. Pink dashed contour outlines the Bayelva catchment.

2. Study Area

Spitsbergen is the largest island of the Svalbard archipelago, Arctic Ocean. Its western coast is characterized by various large glacial fjord systems including the Kongsfjord. The Kongsfjord covers an area of approximately 231 km^2 with a maximum depth of 400 m. Several sub basins characterize the bathymetry of the fjord and since it does not have a sill at the fjord mouth restricting water mass exchange, the water column is permanently oxic (Blinova et al., 2012; Howe et al., 2003; H. Svendsen et al., 2002). Surface water derived from summer glacial freshwater run-off, ice calving, snowmelt, and precipitation overlies cold Arctic Water supplied from the East Spitsbergen Current. Underneath, a transitional/mixed water layer referred to as the transformed Arctic Water separates the Arctic water body from warmer Atlantic bottom water supplied from the West Spitsbergen Current (Nilsen et al., 2008; Rasmussen et al., 2013; H. Svendsen et al., 2002). The water column stratification is very stable during summer when the fjord is ice-free, but waters are well mixed during winters when the fjord is covered by ice. Historically, sea ice lasted approximately 7–9 months per year, but more recently the inflow of Atlantic water has prevented sea ice formation or reduced its spatial extent and thickness (Cottier et al., 2007; Pavlova et al., 2019).

The Bayelva River, Ny-Ålesund area, Brøgger Peninsula (Figure 1), drains an approximately 32 km^2 large catchment into the Kongsfjord. More than 50% of its catchment is glaciated by the West and East Brøgger glaciers (Vestre and Austre Brøggerbreen) and runoff is limited to June–September at the time of maximum ice melt and permafrost thaw depth (Nowak & Hodson, 2013). The river flows on a bedrock of moraine and terminates in a sandur consisting of boulders and gravel (Bogen & Bønsnes, 2003). The Bayelva catchment is underlain by permafrost with active layer depths of ~0.5–1.5 m (Boike et al., 2018; Nowak & Hodson, 2013). These permafrost soils develop on sedimentary rocks from the Late Paleozoic (conglomerates, sandstones, carbonate rocks, cherts, and siliceous limestones) as well as the Cenozoic (conglomerates, sandstones, and shales), the latter characterized by interbedded coal seams that were mined from 1916 to 1962 (Orvin, 1934; H. Svendsen et al., 2002). Pedogenesis is weak and soils are characterized primarily as haplorthels with high lithic and low nutrient content (Wojcik et al., 2019). The vegetation growing on permafrost in the Ny-Ålesund area, a polar semi-desert, during summer is dominated by bryophytes (mosses and lichens), which account for approximately 50% of the total surface area. Vascular plants follow a successional pattern with distance from the glacier and cover up to ~20%–30% of the total surface area. The most prominent vascular plant species include *Saxifraga oppositifolia*, *Dryas octopetala*, *Salix polaris*, and *Luzula confusa* while *Drepanocladus* spp. and *Cetraria delisei* are the most abundant moss and lichen species, respectively (Brossard & Joly, 1994; LLoyd, 2001; Muraoka et al., 2008). The growing period of vascular plants is short, lasting from June to August, while mosses and lichens persist from spring until autumn (LLoyd, 2001).

Table 1
Sample Locations

Station	Sample name	Latitude (°N)	Longitude (°E)	Elevation (m)	Sampling year
LH	Leirhaugen soil	78.92377	11.83810	38.0	2007
KH	Kolhaugen soil	78.92447	11.85750	45.0	2007
UDA	Upper Drainage Area soil	78.92550	11.88416	33.0	2007
LDA	Lower Drainage Area soil	78.92861	11.84138	14.0	2007
BY-R	Bayelva River	78.93433	11.84600	sea level	2008
WP280	Bayelva river mouth	78.93333	11.86950	−3.6	2008
Station T	central Kongsfjord	78.98330	11.86920	−330.0	2008

Abbreviations; BY-R, Bayelva River; KH, Kolhaugen; LH, Leirhaugen; LDA, Lower Drainage Area; UDA, Upper Drainage Area

3. Materials and Methods

3.1. Materials

The sampling strategy was designed to obtain an export transect sample set covering the permafrost soil-river-ocean system. Samples were taken during several land- and ship-based campaigns. In 2007, soil samples from the Bayelva River catchment were collected from the thawed active layer in the northern foreland of the East Brøgger glacier (Figure 1, Table 1). Leirhaugen (LH) is adjacent to the main stem of the Bayelva River (Boike et al., 2008) and permafrost ground temperatures have been monitored at this site since 1998 (Boike et al., 2018; Roth & Boike, 2001). Additional soil profiles in the catchment were sampled from Kolhaugen (KH), Upper Drainage Area (UDA), and Lower Drainage Area (LDA) as described by Rethemeyer et al. (2010). Briefly, soil pits (ca. 1.5 m^2) were opened to up to ~1 m depth (Tables S1 and S2) at each site, reaching either the permafrost table or bedrock-like ground that precluded further excavation. All profiles were sub-sampled based on visible redox characteristics (e.g., color), typically representing three mineral soil horizons. Soil samples were stored frozen (−20°C) in precombusted glass jars until analysis. A sample of coal was also obtained from the catchment.

Sediment samples from the Bayelva River (BY-R), its river mouth (WP280), and the central Kongsfjord (Station T) were obtained in 2008 using a shovel (BY-R), push cores operated by divers (WP280; 10 cm total sediment recovery) or a hand-operated HAPS corer (Station T; 14 cm total sediment recovery). All sediment samples were sliced into 0–1 or 0–2 cm segments and stored in precombusted glass jars at −20°C until analysis.

3.2. Methods

Soil samples were sieved through a 2 mm sieve and visible coal particles were removed. Soil and sediment samples were freeze-dried, homogenized, and Soxhlet-extracted for 48 h (following a 24 h cellulose thimble pre-extraction) using a 90:10 dichloromethane: methanol (v:v) solvent mixture (Kusch et al., 2016). The total lipid extract was processed and alkanoic acids were separated from neutral lipids, purified, and converted to fatty acid methyl esters (FAMEs) according to the methods described in Mollenhauer and Eglinton (2007), except $AgNO_3$ column chromatography was performed instead of urea adduction. A split of the fatty acid methyl ester fraction was taken for routine quantitative flame-ionization gas chromatography (GC-FID) analysis, and concentrations were calculated using an external FAME standard mixture. For isolation of FAME homologs, preparative capillary gas chromatography (PCGC) was used according to the method described in Kusch et al. (2010). To remove potential contamination from column bleed, FAMEs were eluted over a silica gel column after isolation using hexane: dichloromethane (2:1 v:v). This PCGC isolation procedure was checked for blank carbon contribution at the time and no significant contamination was detected (Mollenhauer & Rethemeyer, 2009). Based on individual FAME quantities, homologs were pooled and samples were converted to CO_2. FAMEs were transferred into precombusted (900°C) quartz tubes and 150 μg precombusted copper oxide were added as oxygen source. The quartz

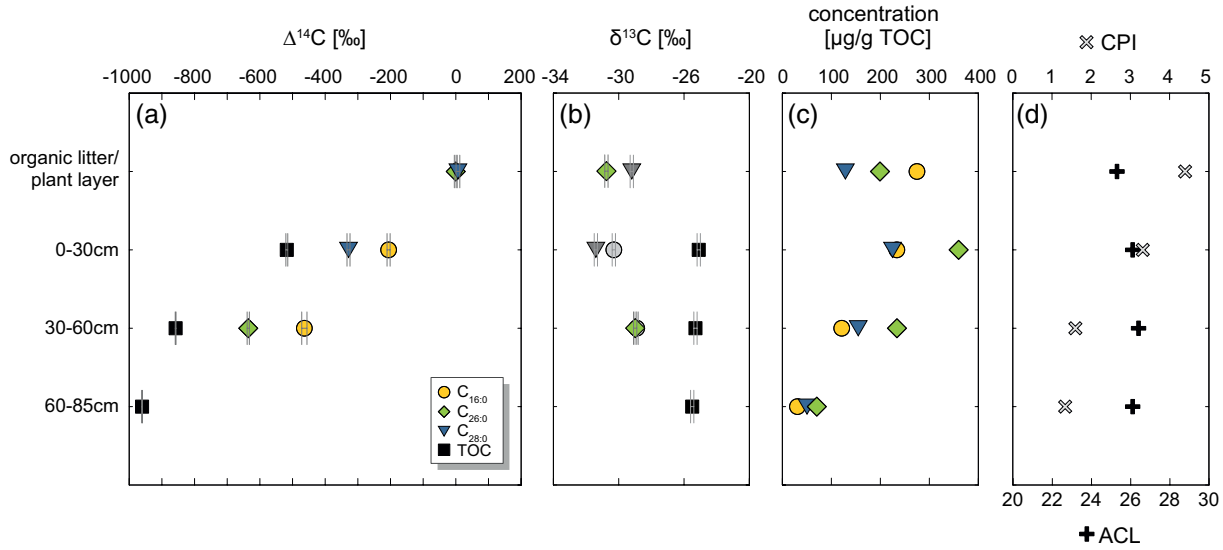

Figure 2. The $\Delta^{14}C$ (a) and $\delta^{13}C$ (b) carbon isotopic composition of bulk OC and alkanoic acids in the Leirhaugen permafrost soil profile. Corresponding concentrations (c) and CPI and ACL (d) of individual alkanoic acids in the profile. Error bars show 1σ analytical uncertainty. ACL, average chain length; CPI, carbon preference index, OC, organic carbon.

tubes were evacuated while immersed in dry ice, flame-sealed, and combusted at 900°C for 4 h. Resulting CO_2 was stripped of water and quantified. Samples were ^{14}C-analyzed at the National Ocean Sciences Accelerator Mass Spectrometry (NOSAMS) Facility at Woods Hole Oceanographic Institution and the CologneAMS facility at the University of Cologne. AMS measurements of bulk OC were carried out using standard methods (McNichol et al., 1994; Rethemeyer et al., 2013), compound-specific AMS radiocarbon measurements were performed following dedicated techniques for small sample sizes (Pearson et al., 1998). Splits of the CO_2 gas samples were used to measure the stable carbon isotopic composition on a VG Optima IRMS. Radiocarbon results are reported as conventional ^{14}C ages in years BP and $\Delta^{14}C$ in ‰ according to Stuiver and Polach (1977), including correction for kinetic fractionation based on $\delta^{13}C$ values. The $\delta^{13}C$ values are reported in ‰ relative to VPDB. Both $\Delta^{14}C$ and $\delta^{13}C$ values of individual alkanoic acids were corrected for the addition of one methyl group during derivatization using isotope mass balance.

4. Results

4.1. Elemental and Molecular Geochemical Data

Organic carbon contents (%OC) in the permafrost soil profiles range from 0.1% to 3.3% (Tables S1 and S2) with the lowest %OC typically observed in the deepest sample of each profile. The organic litter/plant layers have %OC values from 19.9% to 28.4%. Alkanoic acid concentrations in the permafrost soils and organic litter/plant layers show a bimodal distribution with short-chain maxima centering on $C_{16:0}$ or $C_{18:0}$ and long-chain maxima centering on $C_{24:0}$ or $C_{26:0}$. The average chain length (ACL: $[\Sigma n \times C_n]/[\Sigma C_n]$; $n = 16–32$) ranges from 25.3 to 26.4 in the LH profile, 22.7 to 25.0 in the KH trough profile, 24.1 to 25.4 in the KH center profile, 24.7 to 26.3 in the UDA profile, and 25.2 to 27.4 in the LDA profile, respectively. ACL distributions (Figures 2 and S1) do not show a common trend between permafrost profiles. Carbon preference index (CPI: $0.5 \times [\Sigma C_{20–30}/\Sigma C_{19–29} + \Sigma C_{20–30}/\Sigma C_{21–31}]$) values range from 4.4 to 1.4 (LH), 4.4 to 1.5 (KH trough), 1.6 to 2.2 (KH center), 7.0 to 1.8 (UDA), and 3.7 to 3.5 (LDA). Overall, CPI values decrease with depth throughout the profile, but some profiles show a slight increase in the lowermost depth (Figures 2 and S1). CPI values in the mineral soils are consistent with values determined for bacterial biomass (Wiesenberg et al., 2012). Unfortunately, alkanoic acid concentrations in the KH, UDA, and LDA soil profiles (Table S2) were one to two orders of magnitude lower (per gram dry weight) than in LH, thus, restricting compound-specific ^{14}C analyses to LH.

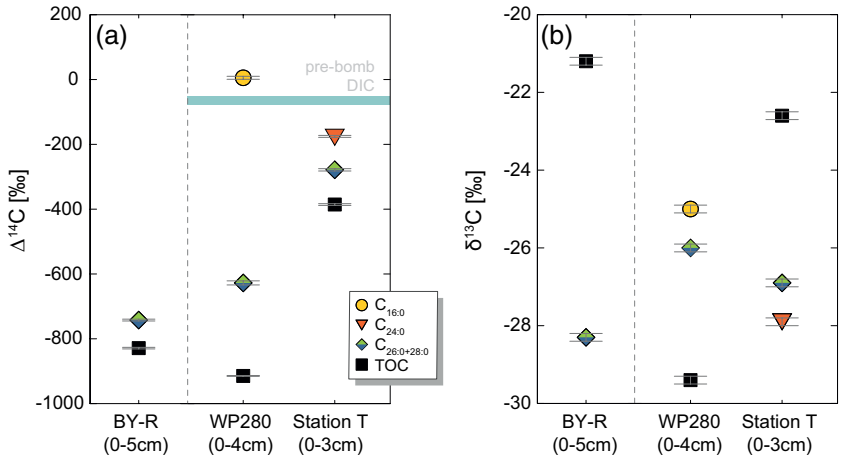

Figure 3. The $\Delta^{14}C$ (a) and $\delta^{13}C$ (b) carbon isotopic composition of bulk OC and alkanoic acids in the Bayelva River and Kongsfjord surface sediments. Note that the pooled long-chain alkanoic acid sample at station WP280 also includes $C_{24:0}$ alkanoic acid and was obtained from 4–6 cm depth. Error bars show 1σ analytical uncertainty. "Pre-bomb DIC" denotes the $\Delta^{14}C$ range of DIC determined for Spitsbergen fjords by Mangerud and Gulliksen (1975). DIC, dissolved inorganic carbon; OC, organic carbon.

Sedimentary %OC ranges from 0.1% (BY-R) to 3.6% (Station T; Tables S1 and S2). Alkanoic acid distributions are also bimodal in the sediments, but short-chain alkanoic acids are significantly more abundant (up to 2 orders of magnitude) than long-chain alkanoic acids in cores WP280 and Station T whereas they are present in similar abundance in BY-R. The high contribution of short-chain alkanoic acids is mirrored in the corresponding ACL values that range from 16.8 (Station T) to 20.9 (WP280 6–8 cm) in the fjord sediments and is 24.9 in sample BY-R. CPI values range from 1.6 (BY-R) to 2.5 (WP280 0–2 cm).

4.2. Bulk OC Isotope Data

Marine surface sediment (0–2 cm) OC $\Delta^{14}C$ data (Figure 3, Table 2) range from −385.7 ± 2.7‰ (Station T) to −914.6 ± 1.0‰ (WP280). OC $\Delta^{14}C$ values at station WP280 decrease further downcore from −914.6 ± 1.0‰ (0–2 cm) to −985.1 ± 1.0‰ (8–10 cm). Similarly, the $\Delta^{14}C$ values from the LH soil profile (Figure 2) decrease with depth from −517.5 ± 2.9‰ (LH 0–30 cm) to −960.8 ± 0.7‰ (LH 60–85 cm). OC from the Bayelva River (BY-R) reflects a $\Delta^{14}C$ value of −828.7 ± 2.4‰.

OC $\delta^{13}C$ values range from −25.1 ± 1.0‰ (0–30 cm) to −25.5 ± 1.0‰ (60–85 cm) in the LH soil profile and are −21.2 ± 1.0‰ in the river sediment (BY-R) and −22.6 ± 1.0‰ at Station T.

4.3. Alkanoic Acid Isotope Data

The $\Delta^{14}C$ value (Figure 3, Table 2) of short-chain $C_{16:0}$ alkanoic acid at station WP280 is −73.3 ± 3.3‰. For the LH soil profile $C_{16:0}$ alkanoic acid $\Delta^{14}C$ values (Figure 2) are significantly more depleted ranging from −205.9 ± 4.7‰ (LH 0–30 cm) to −463.8 ± 8.0‰ (LH 30–60 cm). Long-chain $C_{26:0}$ and $C_{28:0}$ (or combined $C_{26:0+28:0}$) alkanoic acid $\Delta^{14}C$ values range from −278.6 ± 3.6‰ ($C_{26:0+28:0}$; Station T) to −627.5 ± 6.2‰ ($C_{26:0+28:0}$; WP280 4–6 cm). Unfortunately, low alkanoic acid concentrations at 60–85 cm depth precluded CSRA. At all stations where multiple alkanoic acid $\Delta^{14}C$ values are available, $\Delta^{14}C$ values are more depleted with increasing chain length except for $C_{26:0}$ and $C_{28:0}$ in the organic litter/plant layer of the LH soil profile, which agree within 1σ analytical uncertainty.

High molecular weight $C_{26:0}$ and $C_{28:0}$ alkanoic acid $\delta^{13}C$ values range from −29.0 ± 0.1‰ (30–60 cm) to −31.4 ± 0.1‰ (0–30 cm) in the soil profile and the $\delta^{13}C$ value of $C_{26:0+28:0}$ alkanoic acids in the Bayelva sediment is −28.3 ± 0.1‰. In the fjord, HMW alkanoic acid $\delta^{13}C$ values range from −26.0 ± 0.1‰ ($C_{24:0+26:0+28:0}$; WP280 4–6 cm) to −27.9 ± 0.1‰ ($C_{24:0}$; Station T). The $\delta^{13}C$ values of LMW $C_{16:0}$ alkanoic acid in the LH soil profile are −30.3 ± 0.1‰ at 0–30 cm depth and −28.9 ± 0.1‰ at 30–60 cm depth (Table 2) and −25.1 ± 0.1‰ in the Kongsfjord surface sediment. The $C_{24:0}$ alkanoic acid $\delta^{13}C$ value at Station T is −27.9 ± 0.1‰.

Table 2
Radiocarbon and Stable Carbon Isotopic Composition ($\Delta^{14}C$ and $\delta^{13}C$ Given in ‰) of Soil (Leirhaugen), River (Bayelva) and Fjord (Kongsfjord) sediments. Errors Given as 1σ Analytical Uncertainty (Propagated for Alkanoic acids)

Sample	$\Delta^{14}C$ (‰)	^{14}C age (years BP)	$\delta^{13}C$ (‰)	AMS ID No.
Leirhaugen				
LH (organic litter/plant layer)				
$C_{26:0}$ alkanoic acid	−0.2 ± 4.8	bomb-^{14}C	−30.7 ± 0.1	NOSAMS 74182
$C_{28:0}$ alkanoic acid	6.4 ± 6.0	bomb-^{14}C	−29.2 ± 0.1	NOSAMS 74183
LH (0–30 cm)				
$C_{16:0}$ alkanoic acid	−205.9 ± 5.0	1,800 ± 50	−30.3 ± 0.1	NOSAMS 74184
$C_{28:0}$ alkanoic acid	−328.7 ± 4.9	3,140 ± 60	−31.4 ± 0.1	NOSAMS 74185
bulk OC	−517.5 ± 2.9	5,800 ± 50	−25.1 ± 0.1	NOSAMS 66572
LH (30–60 cm)				
$C_{16:0}$ alkanoic acid	−463.8 ± 8.2	4,950 ± 120	−28.9 ± 0.1	NOSAMS 74186
$C_{26:0}$ alkanoic acid	−635.5 ± 3.8	8,050 ± 85	−29.0 ± 0.1	NOSAMS 74187
bulk OC	−858.0 ± 1.3	15,600 ± 70	−25.3 ± 0.1	NOSAMS 66573
LH (60–85 cm)				
bulk OC	−960.8 ± 0.7	26,000 ± 130	−25.5 ± 0.1	NOSAMS 66574
Bayelva River				
BY-R (0–5 cm)				
$C_{26:0+28:0}$ alkanoic acid	−742.1 ± 3.3	10,830 ± 100	−28.3 ± 0.1	NOSAMS 74188
bulk OC	−828.7 ± 2.4	14,100 ± 110	−21.2 ± 0.1	NOSAMS 66576
Kongsfjord				
WP280 (0–4 cm)				
$C_{16:0}$ alkanoic acid[a]	10.4 ± 5.6	bomb-^{14}C	−25.0 ± 0.1	NOSAMS 74189
$C_{16:0}$ alkanoic acid[a]	0.1 ± 4.2	bomb-^{14}C	−25.0 ± 0.1	NOSAMS 74190
bulk OC (0–2 cm)	−914.6 ± 1.0	19,750 ± 130	n.d.	COL1543.1.2
WP280 (4–6 cm)				
$C_{24:0+26:0+28:0}$ alkanoic acid	−628.0 ± 6.5	7,890 ± 140	−26.0 ± 0.1	NOSAMS 74191
bulk OC	−981.1 ± 1.0	31,750 ± 530	n.d.	COL1544.1.2
WP280 (8–10 cm)				
bulk OC	−985.1 ± 1.0	33,700 ± 500	n.d.	COL1545.1.1
Station T (0–3 cm)				
$C_{24:0}$ alkanoic acid	−175.4 ± 3.5	1,490 ± 35	−27.9 ± 0.1	NOSAMS 89091
$C_{26:0+28:0}$ alkanoic acid	−278.6 ± 4.0	2,560 ± 45	−26.9 ± 0.1	NOSAMS 89092
bulk OC	−385.7 ± 2.7	3,850 ± 35	−22.6 ± 0.1	NOSAMS 83355

Errors given as 1σ analytical uncertainty (propagated for alkanoic acids).
Abbreviations: BY-R, Bayelva River; LH, Leirhaugen; n.d., not determined; OC, organic carbon.
[a]Sample was split prior to AMS measurements.

5. Discussion

5.1. Isotope Source Signatures of Permafrost OC in the Bayelva Catchment

The LH soil profile is characterized by bulk OC $\Delta^{14}C$ values that are significantly depleted and decrease with depth (Figure 2, Table S2), a pattern that unlikely reflects long-term radioactive decay of biomass alone, but rather results from the contribution of coal particles to the bulk OC pool (Kim et al., 2011). This interpretation may be supported by the very good agreement of the LH bulk OC $\delta^{13}C$ values (mean −25.3‰) with

the $\delta^{13}C$ value of coal (mean −25.0‰) from the Bayelva catchment analyzed by Kim et al. (2011), although coal-free bulk soil OC or lichen may have similar $\delta^{13}C$ isotopic compositions (Zwolicki et al., 2016). Concurrent compound-specific $\Delta^{14}C$ values of both short-chain $C_{16:0}$ and long-chain $C_{26:0}$ and $C_{28:0}$ alkanoic acids are significantly higher than bulk OC values (confirming coal contributions to bulk OC) but also decrease from the organic litter/plant layer into deeper mineral soil horizons (Figure 2). Rethemeyer et al. (2010) demonstrated that these alkanoic acids derive mainly from bacteria, moss, lichen, and tundra vegetation. However, alkanoic acids have previously also been detected in coal (Baset et al., 1980; Niwa et al., 1988; Snape et al., 1981). The LH alkanoic acid inventories may, thus, contain a coal-derived subpool that may potentially bias $\Delta^{14}C$ values although alkanoic acids have not been reported from coal on Svalbard (Ćmiel & Fabiańska, 2004; Marshall et al., 2015). While we could detect alkanoic acids in the coal sample from the catchment, multiple lines of evidence suggest that the alkanoic acid signature is not authigenic but rather stems from intrusion of modern OC: The overall alkanoic acid concentrations in the coal were much lower than observed in the soil profiles (especially for long-chain homologs) and $C_{16:1}$ and $C_{18:1}$ alkanoic acids had the highest individual concentrations (Table S2). Short-chain monoenoic alkanoic acids degrade during early coalification (Řezanka, 1992) and typically have a microbial origin (Zelles, 1999). Moreover, Svalbard coals are strongly coalified as indicated by high maceral content and high vitrinite reflection classifying them as bituminous coal (Ćmiel & Fabiańska, 2004; Marshall et al., 2015), which commonly only show traces of long-chain alkanoic acids if any (Baset et al., 1980; Niwa et al., 1988; Řezanka, 1992; Snape et al., 1981). In addition, individual $\delta^{13}C$ values of alkanoic acids in the LH profile agree with those in the organic litter/plant layer (Figure 2, Table S2), which represents recently decomposed vegetation as confirmed by the bomb-^{14}C signature of litter/plant layer $C_{26:0}$ and $C_{28:0}$ alkanoic acid. Even if coal-derived long-chain alkanoic acids contributed to the LH alkanoic acid inventories, their influence on the alkanoic acid $\Delta^{14}C$ values should be negligible (as per mass balance) given that the LH alkanoic acid abundances are 1–2 orders of magnitude higher than those observed in the coal sample. Accordingly, the strong ^{14}C-depletion (−205.9 ± 5.0‰ to −635.5 ± 3.8‰) of alkanoic acids in the LH mineral soil with respect to the atmosphere (~50‰) at the time of sampling in 2007 (Levin et al., 2013) implies slow degradation and radioactive decay of biomass, likely due to freeze-locking and less favorable conditions for microorganisms at greater soil depth.

5.2. Permafrost Turnover in the Bayelva Catchment Inferred from Alkanoic Acids

The decrease of alkanoic acid $\Delta^{14}C$ values with depth mirrors globally observed bulk $\Delta^{14}C$ patterns that are attributed to result from the complex interaction of aboveground input, organic matter turnover, and vertical mixing through bioturbation, leaching, and erosion (Mathieu et al., 2015; Shi et al., 2020). Since the permafrost soils in the Bayelva catchment are mostly frozen throughout the year and active layer thaw is limited to the peak summer months, microbial turnover likely dominates these processes since vegetation is sparse and bioturbation is virtually absent. Instead, cryoturbation may lead to OC mixing in permafrost soil (Bockheim, 2007). However, all investigated soil profiles in the Bayelva catchment (LH, KH, UDA, and LDA) indicate little distortion by cryoturbation since bulk OC content (Table S1), alkanoic acid concentrations (Figures 2, and S1), and bacterial intact polar lipid and bacteriohopanepolyol concentrations (Rethemeyer et al., 2010) decrease with depth in all profiles rather than showing more random distributions (Bockheim, 2007). This observation is in good agreement with a recent study by Wojcik et al. (2019) who also found little evidence for cryoturbation on the Brøgger Peninsula. Accordingly, the decreasing alkanoic acid $\Delta^{14}C$ values in the LH profile and of OC elsewhere on Svalbard (Cherkinsky, 1996) are consistent with a primary control of freeze-locking and degradation/radioactive decay on OC inventories and $\Delta^{14}C$ values in the Bayelva catchment. Since we cannot unequivocally determine the contribution of coal to bulk OC and its influence on $\Delta^{14}C$ values, we will use the alkanoic acid $\Delta^{14}C$ values to assess turnover in the LH soil and by inference, the Bayelva catchment (assuming the LH biomarker distributions are representative for the catchment, which is supported by the good agreement of biomarker abundances with the KH, UDA, and LDA profiles).

The $C_{16:0}$, $C_{26:0}$, and $C_{28:0}$ alkanoic acid $\Delta^{14}C$ values from 0–30 cm depth or 30–60 cm depth (−205.9 ± 5.0‰ to −635.5 ± 3.8‰) correspond to conventional ^{14}C ages of 1,800 ± 50 to 8,050 ± 85 years BP (Table 2, Figure 4a) implying very slow (multi-millennial) alkanoic acid turnover in the LH mineral soil. Here, we will assess alkanoic acid turnover in the LH mineral soils, a function of input/preservation and output/degradation,

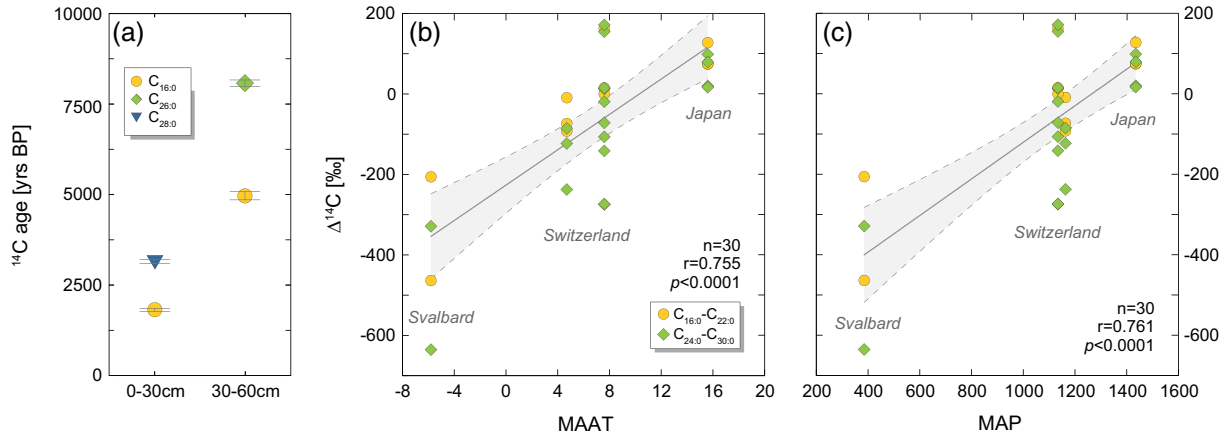

Figure 4. Alkanoic acid radiocarbon ages in the Leirhaugen soil profile (a). Scatter plots of (b) mean annual air temperature (MAAT) and (c) mean annual precipitation (MAP) against the $\Delta^{14}C$ carbon isotopic composition of short-chain and long-chain alkanoic acids (even chain lengths only) in soils from Svalbard (this study), Switzerland (from van der Voort et al., 2017; the subalpine site is characterized by lower MAAT and slightly higher MAP than the temperate site), and Japan (from Matsumoto et al., 2007). In panels (b) and (c), alkanoic acids were grouped according to chain length although data points represent individual homologs except for the pooled $C_{16:0–22:0}$ alkanoic acid samples from Swiss soils; error bars are smaller than symbol size and are omitted for better visibility.

using ^{14}C ages and $\Delta^{14}C$ values rather than calculating turnover times following the approach outlined, for example, by Torn et al. (2009) since the results cannot be reconciled with the environmental history. Turnover time can be calculated assuming either steady state (input flux equals output flux) or open system behavior. While subzero temperatures retain the soils in a state with very limited input and output fluxes throughout most of the year, pedogenesis is likely on-going on the Brøgger Peninsula. However, modeling turnover times for LH with open system behavior (and absence of bomb-^{14}C) requires a soil formation age in considerable excess of the ~10,000 years since deglaciation and emergence of the Brøgger Peninsula (Forman et al., 1987). Modeling alkanoic acid turnover times assuming steady state (i.e., turnover time equals the inverse of the decomposition rate) yields turnover times as high as 14,410 ± 240 years for $C_{26:0}$ alkanoic acid at 30–60 cm depth, thus, also exceeding the Holocene framework for soil development and implying that soils are indeed not at steady state.

Turnover decreases both with depth in the profile and with chain length. In the mineral soil horizons, $C_{16:0}$ alkanoic acid ^{14}C ages increase from 1,800 ± 50 to 4,950 ± 120 and $C_{26:0}$ or $C_{28:0}$ alkanoic acid ^{14}C ages increase from 3,140 ± 60 to 8,050 ± 85 from 0–30 cm to 30–60 cm, respectively (Figure 4a). This pattern has previously been observed in soils by van der Voort et al. (2017) and Matsumoto et al. (2007), the only studies to date reporting compound-specific alkanoic acid ^{14}C data for individual homologs from soils, and may be the result of different sources or different turnover/recalcitrance of individual homologs, or a combination thereof. In soils, long-chain alkanoic acids derive from vascular plants and represent a slow cycling alkanoic acid pool, whereas both vascular plants and microbes are synthesizers (or recyclers) of $C_{16:0}$ alkanoic acid that represents a relatively fast cycling pool (van der Voort et al., 2017), an observation that is confirmed by the LH data. On the Brøgger Peninsula, the organic layer and uppermost 30 cm of soils together store ~80% of the soil OC (Wojcik et al., 2019). Accordingly, the lower turnover of alkanoic acids at depth should primarily result from strongly limited vertical transport of modern OC into the deeper mineral soil and very slow degradation/decomposition rates. In addition, the even shorter thaw period of the deep active layer may further limit/slow down microbial degradation.

While compound-specific $\Delta^{14}C$ values have rarely been determined for soils, the limited information available indicates that alkanoic acid turnover is much faster in non-Arctic regions, analogous to global soil bulk $\Delta^{14}C$ (Shi et al., 2020). Alkanoic acids in one soil sample from Sapporo, Japan all contain bomb-^{14}C indicating decadal turnover (Matsumoto et al., 2007). Short-chain and long-chain alkanoic acids from a temperate soil profile in Switzerland range from 171.5 ± 0.6‰ to −273.7 ± 5.8‰ (van der Voort et al., 2017) with the majority of $\Delta^{14}C$ values containing bomb-^{14}C which implies primarily decadal turnover. In the same study, alkanoic acid $\Delta^{14}C$ values at a subalpine Swiss site range from −9.2 ± 1.2‰ to −274.4 ± 0.4‰ (van der Voort

et al., 2017) indicating centennial to millennial turnover. In comparison with the alkanoic acid $\Delta^{14}C$ values determined for both Swiss locations, the ^{14}C-depletion for the fast ($C_{16:0}$ alkanoic acid) and slow ($C_{26:0}$ and $C_{28:0}$ alkanoic acid) cycling alkanoic acid pools in each soil horizon and between soil horizons is significantly higher in the LH profile.

Globally, both temperature and precipitation are considered the primary factors influencing soil OC turnover, with different relative contributions in different climate regimes (Carvalhais et al., 2014; Chen et al., 2013). Comparison of the alkanoic acid $\Delta^{14}C$ data from Svalbard, Switzerland, and Japan soils with climatic data shows that while the $\Delta^{14}C$ amplitude is quite high at each site depending on alkanoic acid chain length and soil depth, alkanoic acid $\Delta^{14}C$ values decrease with both mean annual air temperature and mean annual precipitation (Figures 4b and 4c). Accordingly, alkanoic acid turnover, that is, output/degradation, increases with temperature and precipitation, in agreement with the global soil OC observations. Given the high vulnerability of the high-Arctic to warming (IPCC, 2013), alkanoic acid/permafrost turnover/degradation may likely accelerate in the Bayelva catchment in the future. Deepening of the active layer has been observed on Svalbard since the 1990s (Christiansen et al., 2010; Isaksen et al., 2007) and daily temperature data from 1998 to 2017 show a 3°C–4°C increase in mean annual soil temperature of the active layer (up to 60 cm depth) and permafrost (ca. 1.4 m depth) on Leirhaugen (Boike et al., 2018). Warmer soil temperatures and an extended summer thaw period will likely promote enhanced microbial activity and turnover.

5.3. Tracing Permafrost OC Export into Sediments

5.3.1. Permafrost OC in the Bayelva River

The seasonally active Bayelva River is characterized by high runoff and sediment load, and bank erosion and sliding are common geomorphological processes along its flow path that likely account for the majority of permafrost export (Bogen & Bønsnes, 2003; Nowak & Hodson, 2014). Fine sediment accumulation is patchy in the Bayelva and primarily derives from the suspended load transported during snowmelt and rain floods (Bogen & Bønsnes, 2003), thus, the BY-R sediment sample represents recently eroded/mobilized material. Bulk OC is strongly ^{14}C-depleted ($-828.7 \pm 2.4‰$) and analogous to the LH samples, likely biased by the contribution of coal particles (Figure 3). Notably, the bulk OC $\delta^{13}C$ value in sample Bayelva River surface sediment sample (BY-R) is much higher (by roughly 4‰) than observations from LH and even the coal investigated by Kim et al. (2011), while the $C_{26:0+28:0}$ alkanoic acid $\delta^{13}C$ value agrees within approximately 1‰–2‰ with alkanoic acid $\delta^{13}C$ values from LH. This pattern suggests another yet also strongly ^{14}C-depleted OC pool contributing to bulk OC in Bayelva River. Given the high runoff and high sediment load (Bogen & Bønsnes, 2003) as well as the ^{14}C-depletion of bulk OC, we consider autotrophic production in the river unlikely. Instead, we suspect that ice-rafted debris (IRD; mean $\delta^{13}C = -22.6‰$ and $\Delta^{14}C = -809‰$) may contribute to the sample (Kim et al., 2011).

The $C_{26:0+28:0}$ alkanoic acids in BY-R are strongly ^{14}C-depleted ($\Delta^{14}C = -742.1 \pm 3.3‰$), in fact, their $\Delta^{14}C$ value is roughly 100‰ lower than that of $C_{26:0}$ alkanoic acid at 30–60 cm depth ($\Delta^{14}C = -635.5 \pm 3.4‰$) in the LH soil profile (Figures 2 and 3). While bulk OC may contain OC from IRD, we do not expect this OC to be a major source of long-chain alkanoic acids to the Bayelva sediment. Glacier OC and runoff is typically dominated by anthropogenic hetero-aromatic aerosols with only minor contribution of saturated hydrocarbons (Grannas et al., 2006; Stubbins et al., 2012). If the Brøgger glaciers indeed contained alkanoic acids, they likely derive from erosion of basal permafrost from the catchment. Both, basal erosion as well as bank erosion of permafrost provide a mechanism for the deposition of a small sediment entity that originates from the deep active layer or permafrost and is characterized by strongly ^{14}C-depleted $C_{26:0+28:0}$ alkanoic acids. As such, the BY-R sample illustrates that ^{14}C-depleted long-chain alkanoic acids from the deep active layer and/or permafrost are effectively exported to the Bayelva River (and consequently further into the Kongsfjord), a mechanism for which direct molecular-level evidence has thus far not been reported.

5.3.2. Permafrost OC in the Kongsfjord

In the Kongsfjord, sedimentary bulk OC consists of a mixture of marine OC, permafrost OC, and fossil OC (coal and IRD) and the relative contributions of each endmember vary spatially within the fjord depending

on the distance to glaciers or rivers, respectively (e.g., Kim et al., 2011). The investigated core-top sediments are of decadal age (Supplement), thus, any ^{14}C-depletion results from supply of ^{14}C-depleted OC rather than sedimentological processes such as nondeposition or erosion. Off the Bayelva River, the core-top sediment bulk OC at station WP280 is strongly ^{14}C-depleted ($\Delta^{14}C = -914.6 \pm 1.0‰$) revealing substantial contributions of OC containing coal particles. The bulk OC ^{14}C-depletion at this particular site is significantly higher than previously observed in Kongsfjord by Kim et al. (2011), who report values ranging from −203‰ to −735‰, and may be explained by the close proximity to the Bayelva River. At Station T, located in the central Kongsfjord, the bulk OC Δ^{14}C value is significantly higher (−385.7 ± 2.7‰), reflecting enhanced contributions from marine OC and reduced input of OC from permafrost and coal. We trace marine OC in the fjord sediments using the compound-specific Δ^{14}C data from short-chain alkanoic acids at station WP280, which predominantly derive from marine phytoplankton and ice algae (Leu et al., 2006; McMahon et al., 2006; Søreide et al., 2008). Although $C_{16:0}$ alkanoic acids also occur in the LH soil samples, they are characterized by significantly higher δ^{13}C and Δ^{14}C values at station WP280 compared to the LH soil $C_{16:0}$ alkanoic acids. Additional support for a marine origin comes from significantly higher $C_{16:0}$ alkanoic acid concentrations and a much lower ACL in the WP280 core-top (17.4; Table S2) than observed in the LH profile (>25.3; Figure 2). The $C_{16:0}$ alkanoic acids off the Bayelva River are enriched in ^{14}C (mean 5.3 ± 4.6‰) with respect to the pre-bomb surface dissolved inorganic carbon Δ^{14}C value of −57 ± 6‰ to −67 ± 9‰ (Figure 3) obtained from several Spitsbergen fjords (Mangerud & Gulliksen, 1975) attesting to deposition after 1950, which is consistent with the independently derived sediment ages.

In contrast to the planktonic short-chain alkanoic acids, permafrost-derived long-chain alkanoic acids are strongly ^{14}C-depleted (Figure 3), particularly the $C_{24:0+26:0+28:0}$ alkanoic acids at station WP280 that have a Δ^{14}C value of −628.0 ± 6.5‰. The Δ^{14}C values in the fjord sediments agree well with the Δ^{14}C values of $C_{28:0}$ alkanoic acid at 30–60 cm depth in the LH profile (−635.5 ± 3.8‰) as well as the BY-R sample (−742.1 ± 3.3‰), but unlikely results from erosion of specific permafrost depth horizons. Instead, the alkanoic acid Δ^{14}C value in the WP280 surface sediment represents the average alkanoic acid Δ^{14}C value of the eroded permafrost depth horizons weighted by their relative volumetric contributions and alkanoic acid inventories. This implies that substantial amounts of deep active layer and/or permafrost must be transported to station WP280. In contrast to $C_{24:0+26:0+28:0}$ alkanoic acids at station WP280, $C_{26:0+28:0}$ alkanoic acids at offshore Station T have a significantly higher Δ^{14}C value (−278.6 ± 4.0‰). This offset may be even more pronounced if the pooled alkanoic acid sample at station WP280 is in part influenced by $C_{24:0}$ alkanoic acid of marine origin (Volkman et al, 1980, 1998), which would likely have a less ^{14}C-depleted signature similar to $C_{24:0}$ alkanoic acid at Station T (Figure 3). Several physical processes may explain the alkanoic acid Δ^{14}C offset observed at both sites. Due to the very close proximity of site WP280 to the Bayelva River, it exclusively receives terrestrial input from the Bayelva catchment. In contrast, Station T may receive input from other permafrost areas such as Blomstrandhalvøya (Figure 1) that may have different alkanoic acid Δ^{14}C signatures than the Bayelva catchment. If Station T indeed accumulates permafrost OC primarily from the Brøgger Peninsula/Bayelva catchment, transport to this site may be by associated with a grain size/sorting effect on alkanoic acid Δ^{14}C values. Previous observations show that alkanoic acid Δ^{14}C values typically increase with grain size (Bao et al., 2018; Yu et al., 2019); however, Bao et al. (2018) also found the opposite trend in Washington Margin sediments. In addition to storing an estimated ~70% of soil OC on the Brøgger Peninsula, the uppermost 30 cm of mineral soil are also characterized by lower fine fraction bulk density (Wojcik et al., 2019) and based on the LH profile, less ^{14}C-depleted $C_{26:0}$ alkanoic acids ($\Delta^{14}C = -328.7 \pm 4.9‰$). Thus, higher density/larger grain size material containing ^{14}C-depleted long-chain alkanoic acids from deeper mineral soils may only be deposited near station WP280 while the lower density/smaller grain size material is preferentially transported to Station T. Finally, sedimentation rates at Station T are lower than at station WP280 and the respective alkanoic acid Δ^{14}C values may to some extent also record a change in permafrost OC erosion associated with the recent soil temperature change in the Bayelva catchment (Boike et al., 2018).

Our data do not allow to unambiguously identify the process responsible for the observed Δ^{14}C offset between $C_{24:0+26:0+28:0}$ alkanoic acids at station WP280 and $C_{26:0+28:0}$ alkanoic acids at Station T. Irrespective, however, our data illustrate that even at the compound-specific level sedimentary Δ^{14}C values of permafrost-derived OC seem to be heterogenous in the Kongsfjord. Accordingly, bulk OC Δ^{14}C values may not only be influenced by varying degrees of coal contributions admixed to permafrost and marine OC, but

also a nonsteady state permafrost OC $\Delta^{14}C$ endmember. If the definition of the permafrost OC $\Delta^{14}C$ endmember is not straightforward, mass balance approaches used to study the relative contribution of different OC sources to Kongsfjord sedimentary OC similar to the approach of Kim et al. (2011) may lead to biased quantitative estimates. This implies that permafrost export (qualitatively and quantitatively) through time should be reconstructed from more than one single sedimentary record. Moreover, additional complications may arise if the permafrost OC $\Delta^{14}C$ endmember varies through time, for example, in response to changes in water mass distribution or circulation influencing hydrodynamic sorting processes or following erosion of different permafrost soil layers in response to changing temperature.

6. Conclusions

In this study, we use compound-specific ^{14}C analysis of alkanoic acids from soils, river, and fjord sediments from the Bayelva catchment and Kongsfjord. Our data demonstrate that bulk OC $\delta^{13}C$ and $\Delta^{14}C$ values from these samples are strongly biased by the contribution of coal particles. In contrast, alkanoic acid $\delta^{13}C$ and $\Delta^{14}C$ values reflect the carbon isotopic composition of vascular plant-derived permafrost OC and reveal that turnover in the Leirhaugen soil profile decreases with depth and is primarily determined by freeze-locking, that is, alkanoic acid ^{14}C ages are a function of limited microbial decomposition and radioactive decay. Depending on alkanoic acid chain length and soil depth, turnover happens on a multi-millennial scale as implied by ^{14}C ages ranging from 1,800 ± 50 years for $C_{16:0}$ alkanoic acid at 0–30 cm depth to 8,050 ± 85 years for $C_{26:0}$ alkanoic acid at 30–60 cm depth and are significantly longer than in other environments. Long-chain alkanoic acid $\Delta^{14}C$ values allow tracing the export of permafrost OC into the Bayelva River and Kongsfjord sediments. Their sedimentary isotope composition reveals that substantial amounts of deep active layer/permafrost OC are deposited off the Bayelva river mouth. Significant $\Delta^{14}C$ offsets between alkanoic acids in near-shore and offshore sediments reveals that sediments in the central fjord either receive input from other permafrost areas or are affected by sediment sorting (grain size/density effects) and accumulation rates.

Conflict of Interest

The authors declare no conflict of interests.

Acknowledgments
The authors thank Birgit Meyer-Schack, Ralph Kreutz, and Ingrid Stimac for their help during sample processing. The authors highly appreciate the help of Bob Bolton (now at University of Alaska Fairbanks) and the AWIPEV technical divers Max Schwanitz & Crew during sampling. The authors thank Casey Hubert (now at University of Calgary) for providing the Station T sediment sample and the NOSAMS and CologneAMS staff for ^{14}C measurements. This work was funded by the Helmholtz Young Investigator Group "Applications of molecular ^{14}C analysis for the study of sedimentation processes and carbon cycling in marine sediments." Sampling was supported by funding from DFG (MO1416/5). D. Ransby was funded through DFG-Research Center/Cluster of Excellence "The Ocean in the Earth System" and she appreciates the support provided by GLOMAR, Bremen International Graduate School for Marine Sciences. The authors thank Rienk Smittenberg and one anonymous reviewer for their constructive reviews and the editor Miguel Goñi for handling the manuscript.

Data Availability Statement

The data presented in this manuscript are archived in the PANGAEA data repository (Kusch et al., 2020).

References

Bao, R., Uchida, M., Zhao, M., Haghipour, N., Montlucon, D., McNichol, A., et al. (2018). Organic carbon aging during across-shelf transport. *Geophysical Research Letters*, *45*, 8425–8434. https://doi.org/10.1029/2018GL078904

Baset, Z. H., Pancirov, R. J., & Ashe, T. R. (1980). Organic compounds in coal: Structure and origins. *Physics and Chemistry of the Earth*, *12*, 619–630.

Biskaborn, B. K., Smith, S. L., Noetzli, J., Matthes, H., Vieira, G., Streletskiy, D. A., et al. (2019). Permafrost is warming at a global scale. *Nature Communications*. *10*, 1–11.

Blinova, M., Faleide, J. I., Gabrielsen, R. H., & Mjelde, R. (2012). Seafloor expression and shallow structure of a fold-and-thrust system, Isfjorden, west Spitsbergen. *Polar Research*, *31*, 161–213.

Bockheim, J. G. (2007). Importance of cryoturbation in redistributing organic carbon in permafrost-affected soils. *Soil Science Society of America Journal*, *71*, 1335–1342.

Bogen, J., & Bønsnes, T. E. (2003). Erosion and sediment transport in High Arctic rivers, Svalbard. *Polar Research*, *22*, 175–189.

Boike, J., Ippisch, O., Overduin, P. P., Hagedorn, B., & Roth, K. (2008). Water, heat and solute dynamics of a mud boil. *Geomorphology*, *95*, 61–73.

Boike, J., Juszak, I., Lange, S., Chadburn, S., Burke, E., Overduin, P. P., et al. (2018). A 20-year record (1998–2017) of permafrost, active layer and meteorological conditions at a high Arctic permafrost research site (Bayelva, Spitsbergen). *Earth System Science Data*, *10*, 355–390.

Brossard, T., & Joly, D. (1994). Probability models, remote sensing and field observation: Test for mapping some plant distributions in the Kongsfjord area. *Polar Research*, *13*, 153–161.

Carvalhais, N., Forkel, M., Khomik, M., Bellarby, J., Jung, M., Migliavacca, M., et al. (2014). Global covariation of carbon turnover times with climate in terrestrial ecosystems. *Nature Reviews Microbiology*, *514*, 213–217.

Chen, S., Huang, Y., Zou, J., & Shi, Y. (2013). Mean residence time of global topsoil organic carbon depends on temperature, precipitation and soil nitrogen. *Global and Planetary Change*, *100*, 99–108.

Cherkinsky, A. E. (1996). ^{14}C dating and soil organic matter dynamics in Arctic and Subarctic ecosystems. *Radiocarbon*, *38*, 241–245.
Christiansen, H. H., Etzelmüller, B., Isaksen, K., Juliussen, H., Farbrot, H., Humlum, O., et al. (2010). The thermal state of permafrost in the nordic area during the international polar year 2007–2009. *Permafrost and Periglacial Processes*, *21*, 156–181 Available at http://doi.wiley.com/10.1002/ppp.687
Ćmiel, S. R., & Fabiańska, M. J. (2004). Geochemical and petrographic properties of some Spitsbergen coals and dispersed organic matter. *International Journal of Coal Geology*, *57*, 77–97.
Cory, R. M., Crump, B. C., Dobkowski, J. A., & Kling, G. W. (2013). Surface exposure to sunlight stimulates CO_2 release from permafrost soil carbon in the Arctic. *Proceedings of the National Academy of Sciences*, *110*, 3429–3434.
Cottier, F. R., Nilsen, F., Inall, M. E., Gerland, S., Tverberg, V., & Svendsen, H. (2007). Wintertime warming of an Arctic shelf in response to large-scale atmospheric circulation. *Geophysical Research Letters*, *34*, L18504–5. https://doi.org/10.1029/2007GL029948
Cui, X., Bianchi, T. S., Savage, C., & Smith, R. W. (2016). Organic carbon burial in fjords: Terrestrial versus marine inputs. *Earth and Planetary Science Letters*, *451*, 41–50.
D'Andrea, W. J., Vaillencourt, D. A., Balascio, N. L., Werner, A., Roof, S. R., Retelle, M., et al. (2012). Mild Little Ice Age and unprecedented recent warmth in an 1800-year lake sediment record from Svalbard. *Geology*, *40*, 1007–1010.
Diefendorf, A. F., & Freimuth, E. J. (2017). Extracting the most from terrestrial plant-derived n-alkyl lipids and their carbon isotopes from the sedimentary record: A review. *Organic Geochemistry*, *103*, 1–21.
Drenzek, N. J., Montluçon, D. B., Yunker, M. B., Macdonald, R. W., & Eglinton, T. I. (2007). Constraints on the origin of sedimentary organic carbon in the Beaufort Sea from coupled molecular ^{13}C and ^{14}C measurements. *Marine Chemistry*, *103*, 146–162.
Dutta, K., Schuur, E. A. G., Neff, J. C., & Zimov, S. A. (2006). Potential carbon release from permafrost soils of Northeastern Siberia. *Global Change Biology*, *12*, 1–16.
Eglinton, G., & Hamilton, R. J. (1967). Leaf epicuticular waxes. *Science*, *156*, 1322–1335.
Feng, X., Vonk, J. E., Van Dongen, B. E., Gustaffson, Ö., Semiletov, I. P., Dudarev, O. V., et al. (2013). Differential mobilization of terrestrial carbon pools in Eurasian Arctic river basins. *Proceedings of the National Academy of Sciences*, *110*, 14168–14173.
Førland, E. J., Benestad, R., Hanssen-Bauer, I., Haugen, J. E., & Skaugen, T. E. (2011). Temperature and precipitation development at Svalbard 1900–2100. *Advances in Meteorology*. *2011*, 893790.
Forman, S. L., Mann, D. H., & Miller, G. H. (1987). Late Weichselian and Holocene relative sea-level history of Bröggerhalvöya, Spitsbergen. *Quaternary Research*, *27*, 41–50.
Grannas, A. M., Hockaday, W. C., Hatcher, P. G., Thompson, L. G., & Mosley-Thompson, E. (2006). New revelations on the nature of organic matter in ice cores. *Journal of Geophysical Research*, *111*, 1392–1410. https://doi.org/10.1029/2005JD006251
Harland, W. B., Pickton, C., Wright, N., Croxton, C. A., Smith, D. G., Cutbill, J. L., et al. (1976). Some coal-bearing strata in Svalbard. *Norsk Polarinstitut Skrifter*, *164*, 7–89. http://hdl.handle.net/11250/174002
Hilton, R. G., Galy, V., Gaillardet, J., Dellinger, M., Bryant, C., O'Regan, M., et al. (2015). Erosion of organic carbon in the Arctic as a geological carbon dioxide sink. *Nature Reviews Microbiology*, *524*, 84–87.
Howe, J. A., Moreton, S. G., Morri, C., & Morris, P. (2003). Multibeam bathymetry and the depositional environments of Kongsfjorden and Krossfjorden, western Spitsbergen, Svalbard. *Polar Research*, *22*, 301–316.
Hugelius, G., Strauss, J., Zubrzycki, S., Harden, J. W., Schuur, E. A. G., Ping, C. L., et al. (2014). Improved estimates show large circumpolar stocks of permafrost carbon while quantifying substantial uncertainty ranges and identifying remaining data gaps. *Biogeosciences*, *11*, 4771–4822.
Humlum, O., Instanes, A., & Sollid, J. L. (2003). Permafrost in Svalbard: A review of research history, climatic background and engineering challenges. *Polar Research*, *22*, 191–215.
IPCC (2013). Climate change 2013: The physical science basis. In T. F. Stocker, D. Qin, G.-K. Plattner, M. Tignor, S. K. Allen, J. Boschung, A. Nauels, Y. Xia, V. Bex, & P. M. Midgley (Eds.), *Contribution of Working Group I to the Fifth Assessment Report of the Intergovernmental Panel on Climate Change*. Cambridge, United Kingdom and New York, NY: Cambridge University Press.
Isaksen, K., Sollid, J. L., Holmlund, P., & Harris, C. (2007). Recent warming of mountain permafrost in Svalbard and Scandinavia. *Journal of Geophysical Research*, *112*, F02S04. https://doi.org/10.1029/2006JF000522
Kim, J. H., Peterse, F., Willmott, V., Kristensen, D. K., Baas, M., Schouten, S., et al. (2011). Large ancient organic matter contributions to Arctic marine sediments (Svalbard). *Limnology & Oceanography*, *56*, 1463–1474.
Koven, C. D., Lawrence, D. M., & Riley, W. J. (2015). Permafrost carbon-climate feedback is sensitive to deep soil carbon decomposability but not deep soil nitrogen dynamics. *Proceedings of the National Academy of Sciences of the United States of America*, *112*, 3752–3757.
Kusch, S., Rethemeyer, J., Hopmans, E. C., Wacker, L., & Mollenhauer, G. (2016). Factors influencing ^{14}C concentrations of algal and archeal lipids and their associated sea surface temperature proxies in the Black Sea. *Geochimica et Cosmochimica Acta*, *188*, 35–57.
Kusch, S., Rethemeyer, J., Ransby, D., & Mollenhauer, G. (2020). Organic geochemistry, carbon isotopic composition of alkanoic acids and sediment core dating from permafrost soils and river and fjord sediments the Bayelva catchment and Kongsfjord. *Pangaea*. https://doi.org/10.1594/PANGAEA.921162
Kusch, S., Rethemeyer, J., Schefuß, E., & Mollenhauer, G. (2010). Controls on the age of vascular plant biomarkers in Black Sea sediments. *Geochimica et Cosmochimica Acta*, *74*, 7031–7047.
Leu, E., Falk-Petersen, S., Kwaśniewski, S., Wulff, A., Edvardsen, K., & Hessen, D. O. (2006). Fatty acid dynamics during the spring bloom in a High Arctic fjord: importance of abiotic factors versus community changes. *Canadian Journal of Fisheries and Aquatic Sciences*, *63*, 2760–2779.
Levin, I., Kromer, B., & Hammer, S. (2013). Atmospheric $\Delta^{14}CO_2$ trend in Western European background air from 2000 to 2012. *Tellus B: Chemical and Physical Meteorology*, *65*, 20092.
LLoyd, C. R. (2001). On the physical controls of the carbon dioxide balance at a high Arctic site in Svalbard. *Theoretical and Applied Climatology*, *70*, 167–182.
Mangerud, J., & Gulliksen, S. (1975). Apparent radiocarbon ages of recent marine shells from Norway, Spitsbergen, and Arctic Canada. *Quaternary Research*, *5*, 263–273.
Marshall, C., Uguna, J., Large, D. J., Meredith, W., Jochmann, M., Friis, B., et al. (2015). Geochemistry and petrology of paleocene coals from Spitzbergen – Part 2: Maturity variations and implications for local and regional burial models. *International Journal of Coal Geology*, *143*, 1–10.
Mathieu, J. A., Hatte, C., Balesdent, J., & Parent, É. (2015). Deep soil carbon dynamics are driven more by soil type than by climate: a worldwide meta-analysis of radiocarbon profiles. *Global Change Biology*, *21*, 4278–4292.

Matsumoto, K., Kawamura, K., Uchida, M., & Shibata, Y. (2007). Radiocarbon content and stable carbon isotopic ratios of individual fatty acids in subsurface soil: Implication for selective microbial degradation and modification of soil organic matter. *Geochemical Journal*, *41*, 483–492.

Maturilli, M., & Kayser, M. (2016). Arctic warming, moisture increase and circulation changes observed in the Ny-Ålesund homogenized radiosonde record. *Theoretical and Applied Climatology*. *130*, 1–17.

McMahon, K. W., Ambrose, W. G. J., Johnson, B. J., Sun, M. Y., Lopez, G. R., Clough, L. M., et al. (2006). Benthic community response to ice algae and phytoplankton in Ny Alesund, Svalbard. *Marine Ecology Progress Series*, *310*, 1–14.

McNichol, A. P., Osborne, E. A., Gagnon, A. R., Fry, B., & Jones, G. A. (1994). TIC, TOC, DIC, DOC, PIC, POC – unique aspects in the preparation of oceanographic samples for ^{14}C-AMS. *Nuclear Instruments and Methods in Physics Research B*, *92*, 162–165.

Meyer, V. D., Hefter, J., Köhler, P., Tiedemann, R., Gersonde, R., Wacker, L., et al. (2019). Permafrost-carbon mobilization in Beringia caused by deglacial meltwater runoff, sea-level rise and warming. *Environmental Research Letters*, *14*, 085003.

Mollenhauer, G., & Eglinton, T. I. (2007). Diagenetic and sedimentological controls on the composition of organic matter preserved in California Borderland Basin sediments. *Limnology & Oceanography*, *52*, 558–576.

Mollenhauer, G., & Rethemeyer, J. (2009). Compound-specific radiocarbon analysis – Analytical challenges and applications. *IOP Conference Series: Earth and Environmental Science*, *5*, 1–9.

Muraoka, H., Noda, H., Uchida, M., Ohtsuka, T., Koizumi, H., & Nakatsubo, T. (2008). Photosynthetic characteristics and biomass distribution of the dominant vascular plant species in a high Arctic tundra ecosystem, Ny-Ålesund, Svalbard: implications for their role in ecosystem carbon gain. *Journal of Plant Research*, *121*, 137–145.

Nilsen, F., Cottier, F., Skogseth, R., & Mattsson, S. (2008). Fjord-shelf exchanges controlled by ice and brine production: the interannual variation of Atlantic Water in Isfjorden, Svalbard. *Continental Shelf Research*, *28*, 1838–1853.

Niwa, Y., Yumura, M., Ishikawa, K., Kuriki, Y., & Kawamura, M. (1988). Structural identifications of straight-chain fatty-acids and esters in coal extracts by linked scanning mass-spectrometry. *Fuel*, *67*, 98–103.

Nowak, A., & Hodson, A. (2013). Hydrological response of a high-Arctic catchment to changing climate over the past 35 years: A case study of Bayelva watershed, Svalbard. *Polar Research*, *32*, 19691.

Nowak, A., & Hodson, A. (2014). Changes in meltwater chemistry over a 20-year period following a thermal regime switch from polythermal to cold-based glaciation at Austre Brøggerbreen, Svalbard. *Polar Research*, *33*, 399–419.

Orvin, A. K. (1934). *Geology of the Kings Bay region, Spitsbergen: With special reference to the coal deposits*. Oslo.

Pavlova, O., Gerland, S., & Hop, H., (2019). Changes in sea-ice extent and thickness in Kongsfjorden, Svalbard (2003–2016). In Hop, H., & Wiencke, C. (Eds.), *The Ecosystem of Kongsfjorden, Svalbard* (pp. 105–136). Cham: Springer International Publishing.

Pearson, A., McNichol, A. P., Schneider, R. J., von, R. F., & Zheng, Y. (1998). Microscale AMS ^{14}C measurement at NOSAMS. *Radiocarbon*, *40*, 61–75.

Rasmussen, T. L., Forwick, M., & Mackensen, A. (2013). Reprint of: Reconstruction of inflow of Atlantic Water to Isfjorden, Svalbard during the Holocene: Correlation to climate and seasonality. *Marine Micropaleontology*, *99*, 18–28.

Rethemeyer, J., Fülöp, R. H., Höfle, S., Wacker, L., Heinze, S., Hajdas, I., et al. (2013). Status report on sample preparation facilities for ^{14}C analysis at the new CologneAMS center. *Nuclear Instruments and Methods in Physics Research B*, *294*, 168–172.

Rethemeyer, J., Schubotz, F., Talbot, H. M., Cooke, M. P., Hinrichs, K.-U., & Mollenhauer, G. (2010). Distribution of polar membrane lipids in permafrost soils and sediments of a small high Arctic catchment. *Organic Geochemistry*, *41*, 1130–1145.

Řezanka, T. (1992). Identification of very-long-chain acids from peat and coals by capillary gas chromatography-mass spectrometry. *Journal of Chromatography A*, *627*, 241–245.

Romanovsky, V. E., Drozdov, D. S., Oberman, N. G., Malkova, G. V., Kholodov, A. L., Marchenko, S. S., et al. (2010). Thermal state of permafrost in Russia. *Permafrost and Periglacial Processes*, *21*, 136–155.

Roth, K., & Boike, J. (2001). Quantifying the thermal dynamics of a permafrost site near Ny-Ålesund, Svalbard. *Water Resources Research*, *37*, 2901–2914. https://doi.org/10.1029/2000WR000163

Schädel, C., Bader, M. K. F., Schuur, E. A. G., Biasi, C., Bracho, R., Čapek, P., et al. (2016). Potential carbon emissions dominated by carbon dioxide from thawed permafrost soils. *Nature Climate Change*, *6*, 950–953.

Schädel, C., Schuur, E. A. G., Bracho, R., Elberling, B., Knoblauch, C., Lee, H., et al. (2013). Circumpolar assessment of permafrost C quality and its vulnerability over time using long-term incubation data. *Global Change Biology*, *20*, 641–652.

Schuur, E. A. G., Vogel, J. G., Crummer, K. G., Lee, H., Sickman, J. O., & Osterkamp, T. E. (2009). The effect of permafrost thaw on old carbon release and net carbon exchange from tundra. *Nature Reviews Microbiology*, *459*, 556–559.

Shi, Z., Allison, S. D., He, Y., Levine, P. A., Hoyt, A. M., Beem-Miller, J., et al. (2020). The age distribution of global soil carbon inferred from radiocarbon measurements. *Nature Geoscience*. *13*, 1–8.

Smith, R. W., Bianchi, T. S., Allison, M., Savage, C., & Galy, V. (2015). High rates of organic carbon burial in fjord sediments globally. *Nature Geoscience*, *8*, 450–453.

Smith, S. L., Romanovsky, V. E., Lewkowicz, A. G., Burn, C. R., Allard, M., Clow, G. D., et al. (2010). Thermal state of permafrost in North America: A contribution to the international polar year. *Permafrost and Periglacial Processes*, *21*, 117–135.

Snape, C. E., Stokes, B. J., & Bartle, K. D. (1981). Identification of straight-chain fatty-acids in coal extracts and their geochemical relation with straight-chain alkanes. *Fuel*, *60*, 903–908.

Søreide, J. E., Falk-Petersen, S., Hegseth, E. N., Hop, H., Carroll, M. L., Hobson, K. A., et al. (2008). Seasonal feeding strategies of Calanus in the high-Arctic Svalbard region. *Deep Sea Research Part II: Topical Studies in Oceanography*, *55*, 2225–2244.

Stubbins, A., Hood, E., Raymond, P. A., Aiken, G. R., Sleighter, R. L., Hernes, P. J., et al. (2012). Anthropogenic aerosols as a source of ancient dissolved organic matter in glaciers. *Nature Reviews Microbiology*, *5*, 198–201.

Stuiver, M., & Polach, H. A. (1977). Discussion reporting of ^{14}C data. *Radiocarbon*, *19*, 355–363.

Svendsen, H., Beszczynska Møller, A., Hagen, J. O., Lefauconnier, B., Tverberg, V., Gerland, S., et al. (2002). The physical environment of Kongsfjorden–Krossfjorden, an Arctic fjord system in Svalbard. *Polar Research*, *21*, 133–166.

Tarnocai, C., Canadell, J. G., Schuur, E. A. G., Kuhry, P., Mazhitova, G., & Zimov, S. (2009). Soil organic carbon pools in the northern circumpolar permafrost region. *Global Biogeochemical Cycles*, *23*, GB2023.

Torn, M. S., Swanston, C. W., Castanha, C., & Trumbore, S. E. (2009). Storage and turnover of organic matter in soil. In N. Senesi, B. Xing, & P. M. Huang (Eds.), *Biophysico-Chemical Processes Involving Natural Nonliving Organic Matter in Environmental Systems* (pp. 219–272).

van der Voort, T. S., Zell, C. I., Hagedorn, F., Feng, X., McIntyre, C. P., Haghipour, N., et al. (2017). Diverse soil carbon dynamics expressed at the molecular level. *Geophysical Research Letters*, *44*, 11840–11850. https://doi.org/10.1002/2017GL076188

Volkman, J. K., Barrett, S. M., Blackburn, S. I., Mansour, M. P., Sikes, E. L., & Gelin, F. (1998). Microalgal biomarkers: A review of recent research developments. *Organic Geochemistry*, *29*, 1163–1179.

Volkman, J. K., Johns, R. B., Gillan, F. T., Perry, G. J., & Bavor, H. J. (1980). Microbial lipids of an intertidal sediment—I. Fatty acids and hydrocarbons. *Geochimica et Cosmochimica Acta*, *44*, 1133–1143.

Vonk, J. E., Mann, P. J., Davydov, S., Davydova, A., Spencer, R. G. M., Schade, J., et al. (2013). High biolability of ancient permafrost carbon upon thaw. *Geophysical Research Letters*, *40*, 2689–2693. https://doi.org/10.1002/grl.50348

Vonk, J. E., Sánchez-García, L., van Dongen, B. E., Alling, V., Kosmach, D., Charkin, A., et al. (2012). Activation of old carbon by erosion of coastal and subsea permafrost in Arctic Siberia. *Nature*, *489*, 137–140.

Waldrop, M. P., Wickland, K. P., White, R., III, Berhe, A. A., Harden, J. W., & Romanovsky, V. E. (2010). Molecular investigations into a globally important carbon pool: Permafrost-protected carbon in Alaskan soils. *Global Change Biology*, *16*, 2543–2554.

Wiesenberg, G. L. B., Schneckenberger, K., Schwark, L., & Kuzyakov, Y. (2012). Use of molecular ratios to identify changes in fatty acid composition of *Miscanthus X giganteus* (Greef et Deu.) plant tissue, rhizosphere and root-free soil during a laboratory experiment. *Organic Geochemistry*, *46*, 1–11.

Winterfeld, M., Laepple, T., & Mollenhauer, G. (2015). Characterization of particulate organic matter in the Lena River delta and adjacent nearshore zone, NE Siberia – Part I: Radiocarbon inventories. *Biogeosciences*, *12*, 3769–3788.

Winterfeld, M., Mollenhauer, G., Dummann, W., Köhler, P., Lembke-Jene, L., Meyer, V. D., et al. (2018). Deglacial mobilization of pre-aged terrestrial carbon from degrading permafrost. *Nature Communications*, *9*, 3666.

Wojcik, R., Palmtag, J., Hugelius, G., Weiss, N., & Kuhry, P. (2019). Land cover and landform-based upscaling of soil organic carbon stocks on the Brøgger Peninsula, Svalbard. *Arctic Antarctic and Alpine Research*, *51*, 40–57.

Yu, M., Eglinton, T. I., Haghipour, N., Montluçon, D. B., Wacker, L., Wang, Z., et al. (2019). Molecular isotopic insights into hydrodynamic controls on fluvial suspended particulate organic matter transport. *Geochimica et Cosmochimica Acta*, *262*, 78–91.

Zelles, L. (1999). Fatty acid patterns of phospholipids and lipopolysaccharides in the characterization of microbial communities in soil: a review. *Biology and Fertility of Soils*, *29*, 111–129.

Zimov, S. A., Davydov, S. P., Zimova, G. M., Davydova, A. I., Schuur, E. A. G., Dutta, K., et al. (2006). Permafrost carbon: Stock and decomposability of a globally significant carbon pool. *Geophysical Research Letters*, *33*, L20502–5. https://doi.org/10.1029/2006GL027484

Zwolicki, A., Zmudczyńska-Skarbek, K., Richard, P., & Stempniewicz, L. (2016). Importance of marine-derived nutrients supplied by planktivorous seabirds to high Arctic tundra plant communities. *PloS One*, *11*, e0154950–16.